Correlations and Counting Statistics of an Atom Laser

Anton Öttl, Stephan Ritter, Michael Köhl,* and Tilman Esslinger

Institute of Quantum Electronics, ETH Zürich, Hönggerberg, CH–8093 Zürich, Switzerland

(Received 28 July 2005; published 26 August 2005)

We demonstrate time-resolved counting of single atoms extracted from a weakly interacting Bose-Einstein condensate of ^{87}Rb atoms. The atoms are detected with a high-finesse optical cavity and single atom transits are identified. An atom laser beam is formed by continuously output coupling atoms from the Bose-Einstein condensate. We investigate the full counting statistics of this beam and measure its second order correlation function $g^{(2)}(\tau)$ in a Hanbury Brown–Twiss type experiment. For the monoenergetic atom laser we observe a constant correlation function $g^{(2)}(\tau) = 1.00 \pm 0.01$ and an atom number distribution close to a Poissonian statistics. A pseudothermal atomic beam shows a bunching behavior and a Bose distributed counting statistics.

DOI: 10.1103/PhysRevLett.95.090404 PACS numbers: 03.75.Pp, 05.30.Jp, 07.77.Gx, 42.50.Pq

Correlations between identical particles were first observed by Hanbury Brown and Twiss in light beams [1]. Their idea was that intensity fluctuations and the resulting correlations reveal information about the coherence and the quantum statistics of the probed system. This principle has found applications in many fields of physics [2] such as astronomy [3], high-energy physics [4], atomic physics [5], and condensed matter physics [6,7]. In optics, the reduced intensity fluctuations of a laser have been observed by Arecchi [8] only a few years after its invention, thereby disclosing the extraordinary properties of this light source.

With the realization of Bose-Einstein condensation in dilute atomic gases a novel weakly interacting quantum system is available. The interpretation of a Bose-Einstein condensate representing a single, macroscopic wave function has been supported in numerous experiments highlighting its phase coherence [9–12]. Correspondingly, atom lasers are atomic beams which are coherently extracted from Bose-Einstein condensates [13–16]. Their first order phase coherence has been observed both in space [9] and time [17]. However, only the second order coherence reveals whether atom lasers exhibit a truly laserlike behavior. Here we present a measurement of the second order correlation function $g^{(2)}(\tau)$ of an atom laser in a Hanbury Brown–Twiss type experiment.

The second order correlation function $g^{(2)}(\tau)$ represents the conditional likelihood for detecting a particle a time τ later than a previously detected particle and quantifies second order coherence [18]. For a thermal source of bosons $g^{(2)}(\tau)$ equals 2 for $\tau = 0$ and decreases to 1 on the time scale of the correlation time which is given by its energy spread. For a coherent source $g^{(2)}(\tau) = 1$ holds for all times and therefore intensity fluctuations are reduced to the shot noise limit. Higher order coherence in quantum degenerate samples was so far only studied in the spatial domain where atom-atom interactions reveal the short-distance correlations [19]. In an interferometric measurement $g^{(2)}(r)$ has been determined for elongated, phase-fluctuating condensates [20], and recently spatial correlation effects in expanding atom clouds were observed [21].

We demonstrate detection of single atoms from a weakly interacting quantum gas by employing a high-finesse optical cavity [22–24] (see Fig. 1). Detecting the arrival times of all atoms at the cavity explicitly gives access to the full counting statistics that reveals the atom number distribution function and its statistical moments [25,26]. Determining the full counting statistics goes far beyond a measurement of the intensity correlation function only, because it represents the full statistical information about the quantum state. Despite recent progress, especially in mesoscopic electronic systems [27], the full counting statistics has not been measured for massive particles before. For neutral atoms this quantity is of special interest, since the strength of the interaction does not overwhelm the quantum statistics as it is often the case for electrons.

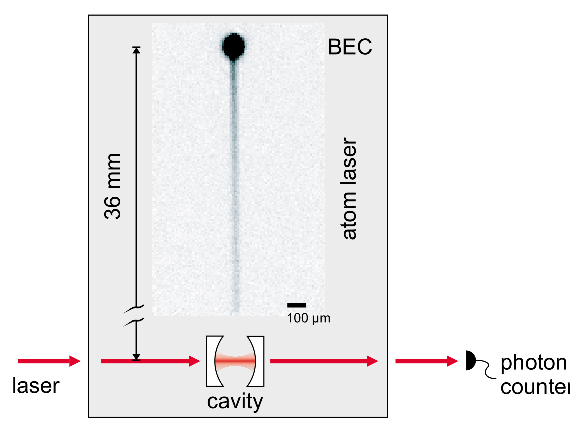

FIG. 1 (color online). Schematic of the experimental setup. A weak continuous atom laser beam is released from a Bose-Einstein condensate. After dropping a distance of 36 mm the atoms enter a high-finesse optical cavity and single atoms in the beam are detected. For the actual measurement the atomic flux is reduced by factor 10^4 as compared to the image.

Our new experimental design combines the techniques for the production of atomic Bose-Einstein condensates with single atom detection by means of a high-finesse optical cavity. The apparatus consists of an ultrahigh vacuum (UHV) chamber which incorporates a separated enclosure with a higher background pressure. Here we collect 10^9 ^{87}Rb atoms in a vapor cell magneto-optical trap which is loaded from a pulsed dispenser source. After polarization gradient cooling and optical pumping into the $|F = 1, m_F = -1\rangle$ hyperfine ground state we magnetically transfer the atoms over a distance of 8 cm out of the enclosure into a magnetic trap. All coils for the magnetic trapping fields are placed inside the UHV chamber and are cooled to below 0 °C. In the magnetic trap we perform radio frequency induced evaporative cooling of the atomic cloud and obtain almost pure Bose-Einstein condensates with 1.5×10^6 atoms. After evaporation we relax the confinement of the atoms to the final trapping frequencies $\omega_\perp = 2\pi \times 29$ Hz and $\omega_\parallel = 2\pi \times 7$ Hz, perpendicular and parallel to the symmetry axis of the magnetic trap, respectively.

For output coupling an atom laser beam we apply a weak continuous microwave field to locally spin flip atoms inside the Bose-Einstein condensate into the $|F = 2, m_F = 0\rangle$ state. These atoms do not experience the magnetic trapping potential but are released from the trap and form a well collimated beam which propagates downwards due to gravity [16]. The output coupling is performed near the center of the Bose condensate for a duration of 500 ms during which we extract on the order of 3×10^3 atoms. After dropping a distance of 36 mm the atoms enter the high-finesse optical cavity (see Fig. 1). Fine tuning of the relative position between the atom laser beam and the cavity mode is obtained by tilting the vacuum chamber. We maintain a magnetic field along the trajectory of the atom laser, which at the position of the cavity is oriented vertically and has a strength of approximately 15 G.

The cavity consists of two identical mirrors separated by 178 μm. Their radius of curvature is 77.5 mm resulting in a Gaussian TEM_{00} mode with a waist of $w_0 = 26$ μm. The coupling strength between a single Rb atom and the cavity field is $g_0 = 2\pi \times 10.4$ MHz on the $F = 2 \rightarrow F' = 3$ transition of the D_2 line. The cavity has a finesse of 3×10^5 and the decay rate of the cavity field is $\kappa = 2\pi \times 1.4$ MHz. The spontaneous emission rate of the rubidium atom is $\Gamma = 2\pi \times 6$ MHz. Therefore we operate in the strong coupling regime of cavity QED. The cavity mirrors are mounted inside a piezo tube which enables precise mechanical control over the length of the resonator [23]. Four radial holes in the piezo element allow atoms to enter the cavity volume and also provide optical access perpendicular to the cavity axis. The cavity resides on top of a vibration isolation mount which ensures excellent passive stability. The cavity resonance frequency is stabilized by means of a far-detuned laser with a wavelength of 831 nm using a Pound-Drever-Hall locking scheme.

The cavity is probed by a weak, near resonant laser beam, whose transmission is monitored by a single photon counting module. The presence of an atom inside the cavity results in a drop of the transmission (see Fig. 2). The stabilization light is blocked from the single photon counter by means of optical filters with an extinction of 120 dB. The probe laser and the cavity are red detuned from the atomic $F = 2 \rightarrow F' = 3$ transition by 40 MHz and 41 MHz, respectively. The polarization of the laser is aligned horizontally and the average intracavity photon number is 5. These settings are optimized to yield a maximum detection efficiency for the released atoms which is $(23 \pm 5)\%$. This number is primarily limited by the size of the atom laser beam which exceeds the cavity mode cross section. The atoms enter the cavity with a velocity of 84 cm/s giving rise to an interaction time with the cavity mode of typically 40 μs, which determines the dead time of our detector. The dead time of our detector is short compared to the time scale of the correlations, which allows us to perform Hanbury Brown–Twiss type measurements with a single detector [28].

We record the cavity transmission for the period of the atom laser operation and average the photon counting data over 20 μs (see Fig. 2). Using a peak detection routine we determine the arrival time of an atom in the cavity, requiring that the cavity transmission drops below its background value by at least 4 times the standard deviation of the photon shot noise. From the arrival times of all atoms we compute the second order correlation function $g^{(2)}(\tau)$ by generating a histogram of all time differences within a single trace and normalizing it by the mean atomic flux. Because of the finite duration of the measurement T, the number of events with a time difference τ is reduced according to $1 - \tau/T$, which is taken into account by dividing the correlation function by this factor. We average

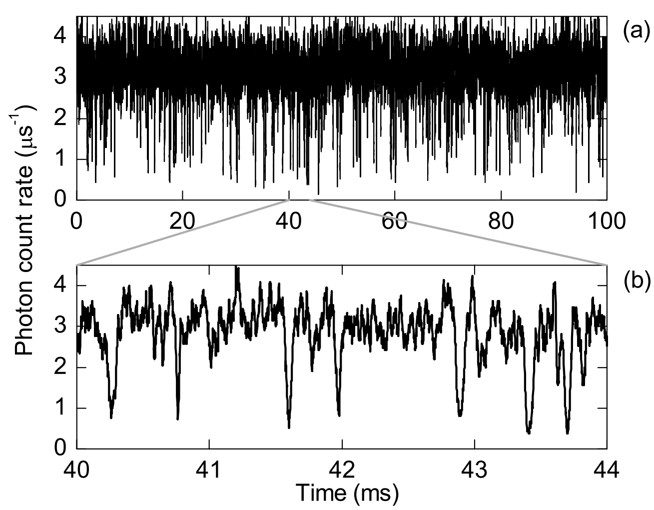

FIG. 2. (a) Light transmission through the high-finesse optical cavity when an atom laser beam is transversing. (b) Details of the single atom transits. The photon count rate is averaged over 20 μs.

these histograms over many repetitions of the experiment to obtain $g^{(2)}(\tau)$ with a high signal-to-noise ratio.

Figure 3(a) shows the measured second order correlation function of an atom laser beam. The value of the correlation function is $g^{(2)}(\tau) = 1.00 \pm 0.01$ which is expected for a coherent source. The second order correlation function being equal to unity reveals the second order coherence of the atom laser beam and is intimately related to the property that it can be described by a single wave function. Residual deviations from unity could arise from technical imperfections. Magnetic field fluctuations either due to current noise in the magnetic trapping coils or due to external fluctuations could imprint small intensity fluctuations onto the atom laser beam. We employ a low noise current source and magnetic shielding to minimize these effects. In addition, we use a highly stable microwave source employing the global positioning system as a frequency reference. A further contribution to a potential modification of the second order correlation function could be due to the output coupling process itself. The spatial correlation function of atoms output coupled from a weakly interacting condensate has been studied theoretically in a situation neglecting gravity [29]. The modification from a constant unity second order correlation function was on the order of 1%, which is on the same order of magnitude as the uncertainty in our data.

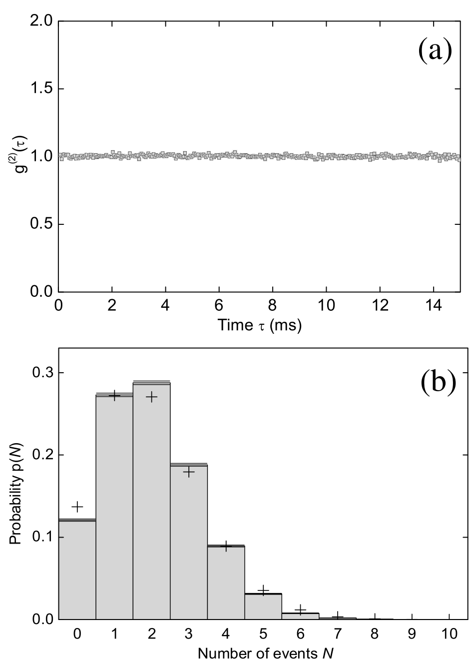

FIG. 3. (a) Second order correlation function of an atom laser beam. The data are binned with a time bin size of 50 μs. The average count number is 2×10^5 per bin. We have omitted the first two data points since they are modified by the dead time of our detector. (b) Probability distribution $p(N)$ of the atom number N detected within a time interval of $T = 1.5$ ms. The (+) symbols show a Poissonian distribution for the same mean value of $\langle n \rangle = 1.99$ as the measured data. The errors indicate statistical errors.

Measuring the second order correlation function requires us to detect the particles within their coherence time and coherence volume [28]. The uncertainty of the detection time of an atom must be smaller than the correlation time, because otherwise the correlations vanish [5]. We estimate that the acquired time delays resulting from a possibly misaligned detector are shorter than the dead time of our detector. It has been measured that the coherence time of the atom laser is given by the duration of output coupling at least for durations of 1.5 ms [17].

Trapped Bose-Einstein condensates have been demonstrated to be phase coherent and to have a uniform spatial and temporal phase [10–12]. The atom laser beam has been theoretically described by a single wave function [29,30] and its spatial coherence was observed [9]. Moreover, a full contrast interference pattern was observed between two atom laser beams extracted from separate locations inside a condensate [12]. This indicates a high degree of spatial overlap between the two propagating modes and a negligible distortion of the uniform spatial phase due to interactions with the remaining condensate. From this we conclude that the atom laser leaves the condensate region with a well defined spatial wave front.

Many overlapping spatial modes at the detector wash out the correlations. In our experimental geometry this is the case when output coupling from a thermal source, since we cannot resolve a single diffraction limited spatial mode. Therefore we do not observe thermal bunching of noncondensed atoms.

Determining the arrival times of all detected atoms explicitly allows us to extract the full counting statistics of the atoms. We choose a time bin length of $T = 1.5$ ms in which we count the number N of detected atoms and plot the probability distribution $p(N)$ [see Fig. 3(b)]. The distribution is close to a Poissonian distribution $p(N) = \langle n \rangle^N e^{-\langle n \rangle}/N!$ with a mean of $\langle n \rangle = 1.99$. For the measured distribution we have calculated the second, third, and fourth cumulant to be $\kappa_2 = 1.75$, $\kappa_3 = 1.34$, and $\kappa_4 = 0.69$, respectively. We attribute the small deviation from the Poissonian distribution to having two or more atoms arriving within the dead time of our detector. For the total flux of 5.2 atoms per ms this probability is 5%.

We realize a direct comparison with a pseudothermal beam of atoms by output coupling a beam with thermal correlations from a Bose-Einstein condensate. This is in close analogy to changing the coherence properties of a laser beam by means of a rotating ground glass disc [8]. Instead of applying a monochromatic microwave field for output coupling we have used a broadband microwave field with inherent frequency and intensity noise. We have employed a white noise generator in combination with quartz crystal bandpass filters which set the bandwidth of the noise. The filters operate at a frequency of a few MHz and the noise signal is subsequently mixed to a fixed frequency signal at 6.8 GHz to match the output coupling frequency. For atomic beams prepared in such a way we

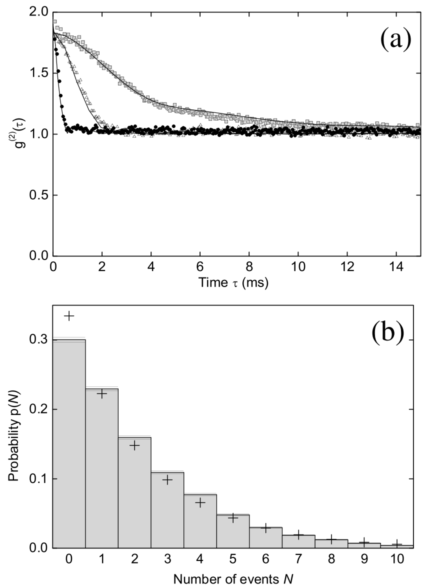

FIG. 4. (a) Second order correlation functions of pseudothermal atomic beams. The square symbols correspond to a filter band width (FWHM) of 90 Hz, the triangles to a bandwidth of 410 Hz, and the circles to a bandwidth of 1870 Hz. The data are binned with a time bin size of 50 μs in which the average count number is 8×10^4. We have omitted the first two data points since they are modified by the dead time of our detector. The lines are the experimentally determined correlation functions of the broadband microwave fields. (b) Probability distribution $p(N)$ of the atom number N within a time interval of $T = 1.5$ ms for the 90 Hz bandwidth data. The (+) symbols indicate a Bose distribution with the same mean value of $\langle n \rangle = 1.99$. The errors indicate statistical errors.

observe bunching with a time constant set by the bandpass filter [see Fig. 4(a)]. To compare our data with the theoretically expected correlation function we have measured the power spectra of the bandpass filters and calculated $|g^{(1)}(\tau)|^2$ of the rf field before frequency mixing. In Fig. 4(a) we plot $1 + \beta|g^{(1)}(\tau)|^2$. The normalization factor $\beta = 0.83$ accounts for the deviation of the experimental data from $g^{(2)}(0) = 2$ due to imperfections in the frequency mixing process.

For the pseudothermal beam we also calculate the counting statistics and find a significantly different behavior than for the atom laser case. For a filter with a spectral width (FWHM) of 90 Hz we have chosen the time bin length of $T = 1.5$ ms, smaller than the correlation time. The atomic flux with a mean atom number $\langle n \rangle = 1.99$ is equal to the case of the atom laser. We compare the measured probability distribution to a Bose distribution $p(N) = \langle n \rangle^N/(1 + \langle n \rangle)^{1+N}$, which is expected for a thermal sample and find good agreement [see Fig. 4(b)]. From the distribution we have extracted the second, third, and fourth cumulant to be $\kappa_2 = 4.6$, $\kappa_3 = 14.5$, and $\kappa_4 = 50.6$, respectively.

In conclusion, we have demonstrated the detection of single atoms from a quantum degenerate source with an efficiency of 23% and measured the second order correlation function of an atom laser. We find the atom laser to be second order coherent. Moreover, the counting statistics of the atom laser was measured and higher moments of the number distribution were extracted.

We would like to thank W. Belzig, T. Bourdel, C. Bruder, T. Donner, A. Frank, G. Morigi, H. Ritsch, T. Stöferle, and J.P. Stucki for discussions and SEP Information Sciences, OLAQUI, and QSIT for funding.

*Email address: Koehl@phys.ethz.ch

[1] R. Hanbury Brown and R. Q. Twiss, Nature (London) **177**, 27 (1956).
[2] G. Baym, Acta Phys. Pol. B **29**, 1839 (1998).
[3] R. Hanbury Brown and R. Q. Twiss, Nature (London) **178**, 1046 (1956).
[4] G. Goldhaber, S. Goldhaber, W. Lee, and A. Pais, Phys. Rev. **120**, 300 (1960).
[5] M. Yasuda and F. Shimizu, Phys. Rev. Lett. **77**, 3090 (1996).
[6] M. Henny *et al.*, Science **284**, 296 (1999).
[7] W. D. Oliver, J. Kim, R. C. Liu, and Y. Yamamoto, Science **284**, 299 (1999).
[8] F. T. Arecchi, Phys. Rev. Lett. **15**, 912 (1965).
[9] M. R. Andrews *et al.*, Science **275**, 637 (1997).
[10] J. Stenger *et al.*, Phys. Rev. Lett. **82**, 4569 (1999).
[11] E. W. Hagley *et al.*, Phys. Rev. Lett. **83**, 3112 (1999).
[12] I. Bloch, T. W. Hänsch, and T. Esslinger, Nature (London) **403**, 166 (2000).
[13] M.-O. Mewes *et al.*, Phys. Rev. Lett. **78**, 582 (1997).
[14] B. P. Anderson and M. A. Kasevich, Science **282**, 1686 (1998).
[15] E. W. Hagley *et al.*, Science **283**, 1706 (1999).
[16] I. Bloch, T. W. Hänsch, and T. Esslinger, Phys. Rev. Lett. **82**, 3008 (1999).
[17] M. Köhl, T. W. Hänsch, and T. Esslinger, Phys. Rev. Lett. **87**, 160404 (2001).
[18] R. Glauber, Phys. Rev. **130**, 2529 (1963).
[19] E. A. Burt *et al.*, Phys. Rev. Lett. **79**, 337 (1997).
[20] D. Hellweg *et al.*, Phys. Rev. Lett. **91**, 010406 (2003).
[21] S. Fölling *et al.*, Nature (London) **434**, 481 (2005); M. Schellekens *et al.*, cond-mat/0508466.
[22] H. Mabuchi, Q. A. Turchette, M. S. Chapman, and H. J. Kimble, Opt. Lett. **21**, 1393 (1996).
[23] P. Münstermann, T. Fischer, P. W. H. Pinkse, and G. Rempe, Opt. Commun. **159**, 63 (1999).
[24] A different technique with the potential of single atom detection in quantum degenerate samples has been demonstrated with metastable helium atoms: A. Robert *et al.*, Science **292**, 461 (2001).
[25] L. S. Levitov, H. Lee, and G. B. Lesovik, J. Math. Phys. (N.Y.) **37**, 4845 (1996).
[26] W. Belzig, C. Schroll, and C. Bruder, cond-mat/0412269.
[27] B. Reulet, J. Senzier, and D. E. Prober, Phys. Rev. Lett. **91**, 196601 (2003).
[28] L. Mandel and E. Wolf, Rev. Mod. Phys. **37**, 231 (1965).
[29] S. Choi, Y. Japha, and K. Burnett, Phys. Rev. A **61**, 063606 (2000).
[30] F. Gerbier, P. Bouyer, and A. Aspect, Phys. Rev. Lett. **86**, 4729 (2001).